thickness) are 2.76×10^{-14} esu and 18.41 μm.[15,19] The calculated $\chi^{(3)}$ values of PPV and PBrPV were 3×10^{-12} esu and 2×10^{-12} esu, respectively. It is well known that $\chi^{(3)}$ value is in inverse proportion to the band gap energy of nonlinear optical media.[20] According to UV-visible spectra in Figure 4, the band gap energy of PBrPV is slightly larger than that of PPV. It is well consistent with the measured $\chi^{(3)}$ values. Conclusively, the introduction of electron-withdrawing bromine atom to PPV is reported to be effective in increasing the band gap due to the decrease in the π-conjugation length, and thus the $\chi^{(3)}$ value of PBrPV film is slightly decreased.

Acknowledgement. It is gratefully acknowledged that this research was supported by the Korea Science and Engineering Foundation.

References

1. Prasad, P. N.; Williams, D. J. *Introduction to Nonlinear Optical Effects in Molecules and Polymers*, John Wiley & Sons, Inc: 1991.
2. Bowden, M. J.; Turner, S. R. *Electronic and Photonic Applications of Polymers*, American Chemical Society: Washington, D. C., 1988.
3. Carter, G. M.; Thakur, M. K.; Chen, Y. J.; Hryniewicz, J. V. *Appl. Phys Lett.* **1985**, *47*, 457.
4. Heeger, A. J.; Moses, D.; Singclair, M. *Synth. Met.* **1986**, *15*, 95.
5. Sauteret, C.; Herman, J-P.; Fray, R.; Pradere, F.; Ducuing, J.; Baughman, R. H.; Chance, R. R. *Phys. Rev. Lett.* **1976**, *36*, 956.
6. Wneck, G. E.; Chien, J. C. W.; Karasz, F. E.; Lillya, C. P. *Polymer.* **1979**, *20*, 1441.
7. Gagnon, D. R.; Capistran, J. D.; Karasz, F. E.; Renz, R. W.; Antoun, S. *Polymer.* **1987**, *28*, 567.
8. Swiatkiewicz, J.; Prasad, P. N.; Karasz, F. E.; Druy, M.; Glatoski, P. *Appl. Phys. Lett.* **1990**, *56*, 892.
9. Kaino, T.; Kubodera, K-I.; Tomaru, S.; Kurihara, T.; Saito, S.; Tsutsui, T.; Tokito, S. *Electronics Letter.* **1987**, *23*, *20*, 1095.
10. Kaino, T.; Kobayashi, H.; Kubodera, K. I.; Kurihara, T.; Saito, S.; Tsutsui, T.; Tokito, S. *Appl. Phys. Lett.* **1989**, *54*, 1619.
11. Shim, H-K.; Hwang, D-H.; Lee, K-S. *Makromol. Chem.* **1993**, *194*, 1115.
12. Shim, H-K.; Hwang, D-H.; Lee, J-I.; Lee, K-S. *Synth. Met.* **1993**, *55*, 908.
13. Liang, W. B.; Renz, R. W.; Karasz, F. E. *J. Polym. Sci. Part A: Polym. Chem.* **1990**, *28*, 2867.
14. Shim, H-K.; Kang, S-W.; Hwang, D-H. *Bull. Korean Chem. Soc.* **1993**, *14*(1), 43.
15. Kubodera, Ken'ichi *Nonlinear Optics*, **1991**, *1*, 71.
16. Kubodera, K.; Kaino, T. *Nonlinear Optics of Organics and Semiconductors, Spring Proceedings in Physics* **1989**, *36*, 163.
17. Kajzar, F.; Messier, J.; Rosilio, C. *J. Appl. Phys.* **1986**, *60*(9), 3040.
18. Tomaru, S.; Kubodera, K.; Zembutsu, S.; Takeda, K.; Hasegawa, M. *Electronic Letters.* **1987**, *23*(11), 595.
19. Buchalter, B.; Meredith, G. R. *Applied Optics* **1982**, *21* (17), 3221.
20. Sauteret, C.; Hermann, J. P.; Frey, R.; Ducuing, J. *Phys. Rev. Lett.* **1976**, *36*, 956.

Single-phase Gallium Nitride on Sapphire with buffering AlN layer by Laser-induced CVD

Jin-Soo Hwang, Sun-Sook Lee, and Paul-Joe Chong*

KRICT, PO BOX 9, Daedeog Science Town, Taejon 305-606

Received July 20, 1993

The laser-assisted chemical vapor deposition (LCVD) is described, by which the growth of single-phase GaN epitaxy is achieved at lower temperatures. Trimethylgallium (TMG) and ammonia are used as source gases to deposit the epitaxial films of GaN under the irradiation of ArF excimer laser (193 nm). The as-grown deposits are obtained on c-face sapphire surface near 700℃, which is substantially reduced, relative to the temperatures in conventional thermolytic processes. To overcome the lattice mismatch between c-face sapphire and GaN ad-layer, aluminum nitride (AlN) is predeposited as buffer layer prior to the deposition of GaN. The gas phase interaction is monitored by means of quadrupole mass analyzer (QMA). The stoichiometric deposition is ascertained by X-ray photoelectron spectroscopy (XPS). The GaN deposits thus obtained are characterized by X-ray diffractometer (XRD), scanning electron microscopy (SEM) and van der Pauw method.

Introduction

Gallium nitride (GaN) is one of the most promising semiconductors for optoelectronic devices, which can be used in the region of blue light emission. It has a direct band gap energy of 3.39 eV.[1] Recently, the electrical and optical properties as well as the crystalline quality of epitaxial GaN film have been improved by introducing a thin buffer layer of

AlN on c-face sapphire.[2] From the use of epitaxial GaN film so obtained, the blue light emitting diodes are fabricated, which demonstrate the highest brightness of 50 mcd at 10 mA/9 V.[3] GaN always has n-type conductivity with high carrier concentration,[4] which is thought to result from nitrogen vacancies[4,5] or oxygen impurity incorporation.[6]

GaN has at least two different crystalline structures.[7] They have generally been known to be wurtzite type structure and zinc-blende type structure of 4 : 4 coordination. Both are likely to occur concurrently as mixed crystal. Wurtzite type α-GaN has the hcp crystal system of AB-type layer structure with puckered rings, and belongs to the space group $P6_3mc$.[8] On the other hand, zinc-blende type β-GaN is the face-centered cubic system with ABC-type layer structure like diamond. The major difference between the two structures is only due to the misoriented configuration of the bonding on tetrahedral atomic sheets. The homo-epitaxial growth of GaN has never been achieved, since GaN has not yet been available in the form of large single crystals.[9] For this reason, various single crystals have been used as substrates in hetero-epitaxial growth of GaN, *e.g.* Si, spinel, GaAs, MgO, SiC and sapphire.[9,10] Among these, the sapphire substrates of c-face (0001), a-face ($11\bar{2}0$) and r-face ($01\bar{1}2$) have been used most widely. However the lattice parameters as well as thermal expansion coefficients are markedly different each other, which gives rise to a major problem. Considering the lattice mismatch of 8.3%, between α-GaN and c-face sapphire,[10] the initial monolayer of a heteroatomic interface would play an important role in determining the growth habits of subsequent layers. Recently, it is reported that the lattice mismatch can be overcome by introducing the buffer layer of wurtzite type, either AlN or ZnO.[11] Both have the same crystal system and similar lattice constant as α-GaN.

Most studies on GaN epitaxy has been performed by means of the thermolytic processes with some improvements, the growth temperature being near or above 1000℃. However, the films of GaN grown by the thermolytic processes have been found to be inadequate as for optoelectronic quality. It is revealed that GaN sublimes near 800℃ and undergoes thermal decomposition above 980℃. It is also suggested that the α-phase crystal is easily transformed to the β-phase at elevated temperatures.[9] With respect to the GaN epitaxial film of better quality, therefore the lowering of the growth temperature has been attempted in recent years. Typical techniques under use in this regard are metal-organic chemical vapour deposition (MOCVD), molecular-beam epitaxy (MBE) or electron cyclotron resonance microwave-plasma-assisted molecular-beam epitaxy (ECR-MBE).[12]

LCVD is an alternative technique, which employs the laser photon in view of selective volume excitation. This is considered to be particularly useful in reducing the thermal instability of GaN deposits. In this study, the ArF excimer laser of 193 nm is employed in order to obtain the single-phase α-GaN epitaxial film on the c-face sapphire substrate with AlN buffer layer. The LCVD study is conducted with assessment of photolytic fragmentation, stoichiometric composition, crystal structure, morphology and electrical properties involved. From the evidence, the characteristics of the laser-assisted deposits are discussed, with an ultimate aim of growing epitaxial GaN films of optoelectronic quality.

Experimental

The LCVD process in use was described elsewhere,[13] and the experimental apparatus was used with minor alteration. The laser-induced deposition was performed in a high vacuum chamber equipped with a turbo molecular pump. The laser photon flux in laminar mode was introduced through a Brewster window into the chamber in parallel with substrate surface. The beam path was adjusted to be *ca.* 15 mm above the substrate. The c-face sapphire was used as substrate which was placed on a resistive-type heater made of tantalum foil. The heater was connected with the power terminals of copper rod extended towards the centre of the vacuum chamber. For monitoring of deposition temperatures, a K-type alumel-chromel thermocouple was installed under the Ta heater. The photon source was a computer-controlled ArF excimer laser of 193 nm (Lambda-Physik, LPX 305 icc). The laser photon was generated in a constant-energy mode at the repetition rate of 50 Hz. For effective 'volume' excitation, the laser beam of 300 mJ per pulse was aligned for use in the current work. With appropriate mirror, iris and/or focusing lens were used as necessary. TMG and ammonia were admitted independently *via* respective tubings of *o.d.* 1/8". Prior to reach of the reaction vessel, they were allowed to mix well in the spirally coiled tubing of *o.d.* 1/8". The flow rates of the reactant gases were regulated by mass flow controllers. The substrate of c-face sapphire was chemically etched in an equimolar mixture of H_2SO_4 and H_3PO_4 at 150-200℃. The wafers were then rinsed thoroughly with deionized water, followed by methanol in an ultrasonic vibrator and allowed to dry.

The laser-induced deposition experiment was conducted as described below. When the wafer-mounted heater was placed in position, the entire chamber was tightly sealed and evacuated to *ca.* 4×10^{-6} Torr. The substrate was then activated at 1050℃ for 30 min with a gentle flow of H_2. Finally, the chamber was pumped down 1.5×10^{-6} Torr. After the substrate reached the deposition temperature of 600± 5 ℃ for AlN buffer layer, further 10 min was allowed to become stabilized. 5 N TMA (Trimethylaluminium) from Strem Chemicals and 5 N ammonia from Matheson were introduced into the reaction chamber at the flow rates of 0.04 and 41.6 sccm, respectively. During the reaction, the total internal pressure was kept constant at 0.9 Torr. When the AlN buffer layer was formed thinly on the sapphire for 3 min, the temperature was raised for the photodeposition of GaN. That was, 6 N TMG (Trimethylgallium) from Strem Chemicals and ammonia were admitted similarly into the chamber at the flow rates of 0.37 and 83.2 sccm, respectively. With laminar photon flux, deposition was performed for 10 min under the internal pressure of 2 Torr. When the deposition was complete, all the gas flows and laser irradiation were shut off. The as-grown deposits were then slowly annealed to 500 ℃ in vacuum, prior to quenching to an ambient temperature.

The resulting GaN deposits were characterized by means of XRD (RIKAGU D/MAX III-B) for the crystal structure and SEM (JEOL JSM 840A) for the surface morphology. SEM was equipped by energy dispersive X-ray spectrometer (EDS), by which the composition of the deposits were analyzed. QMA (Balzers QMA 125) was used for *in-situ* analysis

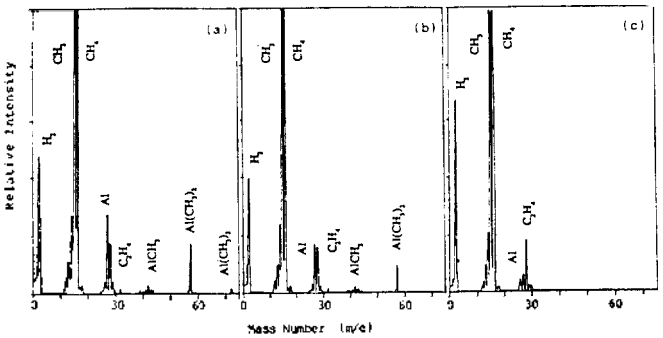

Figure 1. Quadrupole mass spectra for pyrolysis of TMA (a) room temperature (b) 300℃ and (c) 600℃.

of the photofragmented species. For stoichiometric deposition, XPS (VG ESCALAB MK II) was used alternaltely with Al and Mg targets. As necessary, the surface contaminants were etched by argon ion bombardment. The electrical properties of the as-grown deposits were measured by the van der Pauw method, which consists of magnetic housing (Bruker, Magnet B-E 15) and electronic instruments (Picoammeter Model 485, Scanner Model 705 and Current source Model 220, all from Keithley).

Results and Discussion

Comparison of Thermal and Laser-assisted Decomposition. The lower-temperature growth of single-phase epitaxial films of GaN was attempted with introduction of AlN buffer layer by means of a laser-induced CVD technique. As a part of the current studies, the pyrolytic decompositions of NH_3, TMA and TMG were investigated by *in-situ* FT-IR spectroscopy.[14] This was carried out in a closed reactor of cold wall type. Similarly, the pyrolysis of TMG-NH_3 adduct and TMA-NH_3 adduct was also observed. Evidence indicates that the N-H bonds of ammonia are cleaved at about 900℃ but all the rest are completely decomposed in the vicinity of 500℃. In the present work, however, it was not possible to affect the deposition of GaN under 900℃, nor the growth into wurtzite type crystals even at 1000℃. *In-situ* QMA has been made to identify the thermolytic fragments occurring at various temperatures. They may be involved with the formation of AlN buffer layer ad GaN film. Figure 1 shows typical spectra of TMA pyrolysis. TMA is fragmented by the thermal electron from QMA tungsten filament, the spectra obtained at room temperature being as given in Figure 1(a). When the temperature rises beyond 300℃, the fragment ions of Al(mass number; 27), $AlCH_3$(mass number; 42), $Al(CH_3)_2$ (mass number; 57), gradually decrease in their peak intensity as in Figure 1(b). Upon reach of 600℃, these ions completely disappeared as in Figure 1(c). Instead, the peaks due to hydrogen and methane increase to a noticeable extent. The fragmentation patterns of TMG are observed in analogy with those of TMA. The patterns are characterized by the existence of gallium isotope and its ratio. Gallium peaks appear in twins with the isotopes of mass numbers 69 and 71, exactly matching with the natural abundance of 60% and 40%, respectively. This is well evidenced by the peaks of $Ga(CH_3)_2$ occurring in mass numbers of 99, 101, and by those of Ga and $GaCH_3$ occurring in a similar fashion. On the other hand,

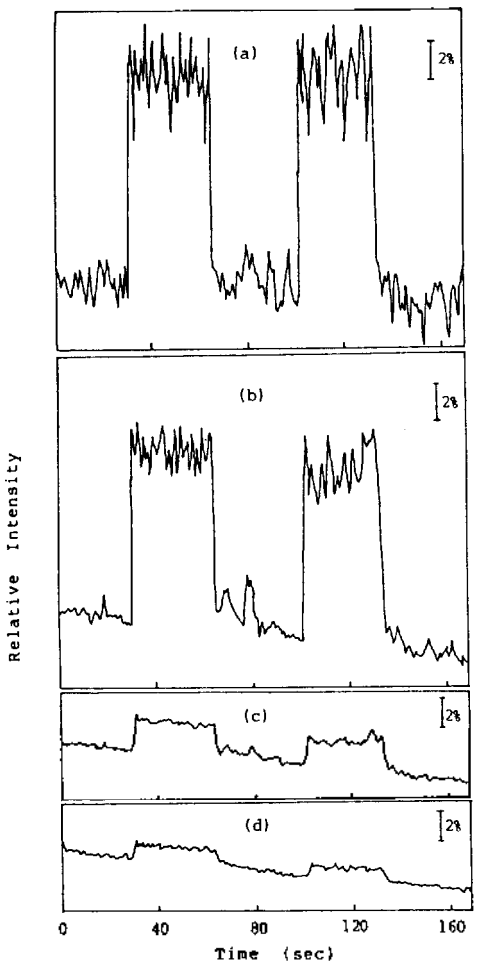

Figure 2. Quadrupole mass spectra for laser stimulated fragmentation of NH_3 molecule (a) N^+ (b) NH^+ (c) NH_2^+ and (d) NH_3^+.

NH_3 is pyrolized at the temperature above 900℃. This is demonstrated by the fact that the peak intensity of hydrogen increases with increasing temperatures above 900℃. *In-situ* FT-IR studies indicate that pyrolytic temperature is different from deposition temperature. In this work, thermal and laser energies were employed simultaneously in order to affect deposition at lower temperatures. The ArF excimer laser was selected since TMG and ammonia can absorb the resonant energy of 193 nm effectively.[15,16] The mean free path of the gaseous species is *ca.* 10 μm. By passing the laser photon flux in parallel to the substrate surface, the molecules in gaseous phase absorbs the photons and are excited. This process permits the photolytic deposition of α-GaN at a relatively low temperature of 700℃. It is found that the TMG molecules are easily fragmented by the laser photon in analogy with their thermolytic instability. Furthermore, the photolysis of ammonia molecules can be enhanced by the laser irradiation even at room temperature.[17] When the ammonia molecules are intermittently irradiated by the laser beam, the mass signals due to the fragments such as N, NH and NH_2, are traced by *in-situ* QMA. The relative abundance of the fragmented species with and without laser irradiations, is compared as given in Figure 2. It shows that the ratio of N (*ca.* 14%) is markedly increased relative to that of other species ($NH \cong 9\%$, $NH_2 \cong 2\%$, $NH_3 \leq 1\%$). This suggests that

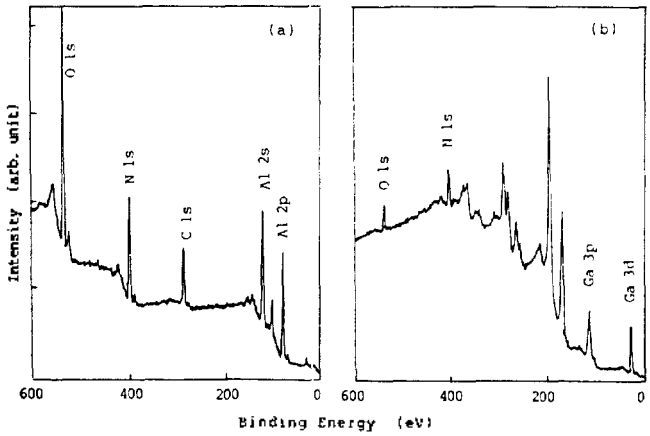

Figure 3. XPS profiles for composition of surface atoms (a) AlN deposits on sapphire as buffer layer (b) laser assisted deposits of GaN.

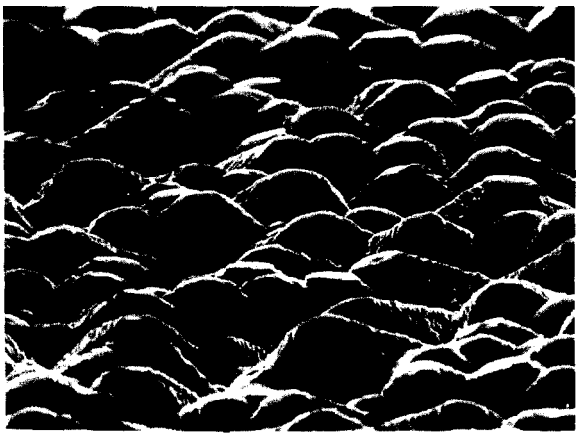

Figure 4. SEM morphology for laser-assisted deposits of α-GaN on c-face sapphire with AlN buffer layer (70° tilt view).

the nascent nitrogen and amidogen species are liberated by the photodissociation, and reactive enough to interact with the surface sites. The laser-induced process is expected not only to accelerate the deposition reaction, but also to reduce the problem of defect inclusion, especially due to thermal instability. This is an unlikely situation with the thermal energy alone.

Stoichiometric Deposition. The crystal structure and surface morphology of GaN deposits are determined by the flow rates of reactant gases. The flow of reactants for stoichiometric deposition are optimized by XPS, so that the equimolar ratios of Al : N and Ga : N may be rendered on the final deposits. Thus, the XPS analysis was carried out for the surface atoms, as shown in Figure 3. For the AlN deposits, the Al-Kα line ($h\nu$ 1486.6 eV) was used as a soft X-ray source, and the resulting data were obtained from 10 times scannings on the two-dimensional surface. The spectral data thus assessed indicate the stoichiometric formation of AlN. It is supposed that the C_{1s} peak near 285 eV may be attributed to the carbonaceous contaiminants and that of O_{1s} near 540 eV may be due to surface oxides. The GaN grown on AlN buffer layer was observed by the Mg-Kα line ($h\nu$ 1253.6 eV), because the gallium peak was imposed with the carbon signals. In case of using the Al-Kα line the same peak was overlapped with the nitrogen signal. Therefore, two sources were employed alternately for analysis of Ga content. Note that the resulting data for GaN reflect not only depth-profile but also two-dimensional surface scans. The deviations of 10-20% are usually involved with quantitative analysis of XPS due to contamination with O_2, CO_2, H_2O in atmosphere. The intense spectral peaks from 170 eV to 390 eV, are shown to split into several energy levels. This corresponds to X-ray fluorescence of Ga LMM line. The GaN deposits exhibit the spectral peaks of C_{1s} and O_{1s} occurring exactly in the same regions as those of AlN layer. Therefore, it is etched by Ar^+ ion bombardment for several minutes. By this, some undefinable surface contaminants are reduced to negligible extent. After etching, the trace carbon signals can be completely removed with subtraction of carbon peak due to some hydrocarbons in vacuum system. With the reactant dosages so adjusted, the as-grown deposits are found to have the binary atomic ratio in proximity of the desired stoichiometry. The specimens obtained in this way were characterized as below.

Morphology. The as-grown deposits are brownish-yellow when produced at lower temperatures. The deposits become pale-yellow at temperatures near 800℃, and dark-yellow at higher temperatures. It is suggested that the color is related to the presence of impurites like carbonaceous intermediates.[18] Typical SEM morphology of GaN deposits is shown in Figure 4. It indicates that the ad-layer is formed with truncated hexagonal 'hillocks'. They are uniaxially oriented, consisting of crystal grains of *ca.* 10 μm in diameter. The growing face of the layer does not look perfectly flat. It is seen that any single hillock doesn't grow predominantly over others. Indication is that the seeds uniformly formed at the nucleation stage undergo inter-growth, resulting in even depth-layer of several μm thickness. It appears that two dimensional surface coverage would be completed in a deposition time of less than 10 min. During the subsequent deposition, the rate of growth is estimated to be *ca.* 500 nm min^{-1}. If the deposition continues for a longer period of time, say 30 min, the hexageonal deposits are likely to become pillared. The initial nucleation appears to proceed very rapidly in a matter of minutes. Undoubtedly, the type of nuclei initially formed will determine the crystal nature of the ad-layers. By the aid of laser photon flux it is believed that the seeding for α-GaN is preferentially induced, so as to have the subsequent growth oriented in the direction perpendicular to the c-axis. In fact, the growth habits and the crystal shapes thus observed are typical of α-GaN, the deposits being regarded as single phase crystallites. On the other hand, the crystals of GaN grown directly on sapphire with no formation of AlN layer were irregular in size.[13] With AlN buffer layer, however, the GaN crystals appear to give three dimensional growth, the entire surface being covered with uniform-size grains. From the EDS analysis, the presence of Ga in the deposits is also confirmed. In addition, the morphology of the ad-layer tends to vary with the growth temperature and with the molar fractions of TMG-NH_3. With the volume ratios in the range of $500<NH_3 : TMG<30$, little de-

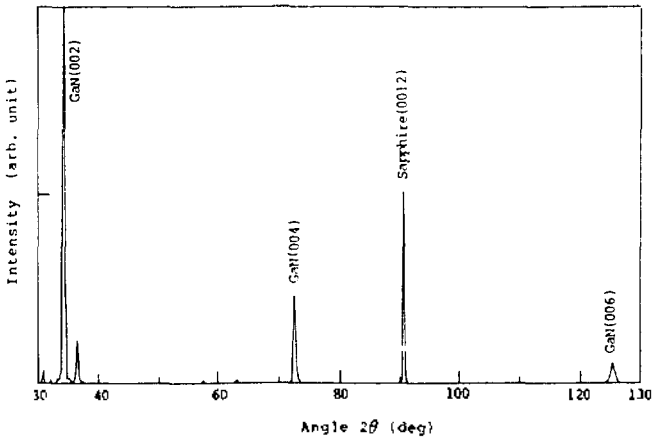

Figure 5. X-ray diffractogram for laser assisted deposits of α-GaN on c-face sapphire with AlN buffer layer.

position occurs even at the growth temperature of 700℃. For crystal perfection, the deposition at higher temperature is by no means desirable, since it may only result in surface roughness. Generally, the thermal energy alone has been considered as unsuitable for the epitaxial growth of GaN films.[13]

Crystal Structure. The sapphire substrate in use belongs to the space group of $R\bar{3}c$, having $a_0=4.758$ Å and $c_0=12.991$ Å. The c-face sapphire has major diffractions at $2\theta=41.72°$, and 90.83° being attributed to (006) and (0012) planes, respectively. Figure 5 shows a typical X-ray diffractogram of the as-grown GaN deposits. For the ad-layers, three major peaks at $2\theta=34.5°$ ($d=2.589$ Å), 72.6° ($d=1.295$ Å) and 125.3° ($d=0.863$ Å) are observed, which are indexed as (002), (004) and (006) faces of the GaN crystal, respectively. The peak at $2\theta=90.83°$ ($d=1.081$ Å) results from (0012) face of the sapphiare, and the minor peak at $2\theta=36.89°$ ($d=2.434$ Å) would be responsible for the (101) face of GaN. The strongest peak at $2\theta=34.38°$ is sharp in appearance with FWHM, relatively narrower than that of GaN grown without AlN buffer. Although the same reflection may be responsible for some misoriented domains due to scattering from (111) planes of β-GaN, the possibility is excluded by the absence of alternative diffractions due to β-GaN. In view of the results as observed from XRD as well as from SEM it is surmised that the crystalline quality is fairly improved by using the AlN layer. For this reason, the resultant deposits are attributed to the wurtzitic structure. The wurtzite type GaN crystal has latttice constants of $a_0=3.186$ Å and $c_0=5.178$ Å, and the bond length of vicinal atoms is 1.942 Å.[8] This is known as the most stable GaN crystal form under ambient conditions. The zinc-blende cubic phase GaN has a lattice constant of 4.51 Å,[4] which is thermodynamically metastable. The XRD data also show a strong indication to have all the (001) planes of α-GaN normal to the c-axis of the substrate. This is in support of the SEM morphology, reflecting that the ad-layers thus formed are well crystallized. All the evidence of XRD as well as SEM indicates fair improvement of GaN cystalline quality with predeposition of AlN buffer layer. When the as-grown depostis are obtained at an elevated temperature, the XRD data become complicated, indicating the occurrence of dentrite-like structure on the (111) plane parallel to the substrate. In previous studies, it is postulated that the crystal formed at relatively higher temperatures may undergo crystal transition from the wurtzite type to the zinc-blende lattice.[9] At temperatures of higher than 1000℃, it is observed that both hexagonal and cubic crystallites are in mixtures on the same substrate. Apart from the thermal transition as denoted above, the hexagonal structure may be transformed to the cubic system, provided that an accidental change in stacking faults is intercepted during the growth.

Electical Properties. Ultimate use of epitaxial GaN films is envisaged as a potential candidate primarily for photo-emissive materials. In this respect it is of interest to evaluate some electronic quality of the GaN deposits as obtained. In fact this would be more relevant than the morphology and the crystal structure alone. It is stated that undoped GaN is always n-type and highly conductive due to a high concentration of nitrogen vacancy.[5,9] It is reported that the carrier concentration is in the range of 4×10^{16}-10^{20} cm^{-3} and Hall mobility in the range of 8-500 $cm^2V^{-1}s^{-1}$. In this study, the computed values of the carrier concentration and Hall mobility at applied current of 0.1 mA and magnetic field of 5000 GAUSS are about 2×10^{18} cm^{-3} and 8 $cm^2V^{-1}s^{-1}$ at room temperature, respectively. The measured carrier density is within the range of the published data,[9] but the mobility is found to be somewhat lower than expected. The relatively low Hall mobility may be caused by the employment of low vapor pressure deposition under use.[9]

Conclusions

The LCVD growth of epitaxial GaN is performed at lower temperatures. The as-grown deposits are obtained at a relatively low temperature near 700℃, being about 300℃ lower than the conventional thermolytic processes. The AlN buffer layer is employed to overcome the lattice mismatch between c-face sapphire and GaN ad-layer. From the results of XRD and SEM, it is found that the crystalline quality is fairly improved by using the AlN buffer. The characterization of the photodeposits indicates the formation of α-GaN crystallites, in spite of some crystal hillocks present. From the results, it is considered that LCVD would be a useful technique in growing the epitaxial films of wurtzite type GaN having an optoelecronic quality.

References

1. Maruska, H. P.; Tietjen, J. J. *Appl. Phys. Lett.* **1969**, *15*, 327.
2. Amano, H.; Sawaki, N.; Akasaki, I.; Toyoda, Y. *Appl. Phys. Lett.* **1986**, *48*, 353.
3. Koide, K.; Kato, H.; Sassa, M.; Yamasaki, S.; Manabe, K.; Hashimoto, M.; Amano, H.; Hiramatsu, K.; Akasaki, I. *J. Cryst. Growth.* **1991**, *115*, 639.
4. Pankove, J. I.; Bloom, S.; Harbeke, G. *RCA Rev.* **1975**, *36*, 163.
5. Nuese, C. J.; Pankove, J. I. *in Topics in Applied Physics*, ed. Pankove, J. I.; Springer-Verlag, New York, **1980**; vol. 40, ch. 2.
6. Seifert, W.; Franzheld, R.; Butter, E.; Sobotta, H.; Riede,

V. *Cryst. Res. Technol.* **1983**, *18*, 383.
7. Lei, T.; Fanciulli, M.; Molnar, R. J.; Moustakas, T. D.; Graham, R. J.; Scanlon, J. *Appl. Phys. Lett.* **1991**, *59*, 944.
8. JCPDS File 2-1078.
9. Elwell, D.; Elwell, M. M. *Prog. Cryst. Growth Charact.* **1988**, *17*, 53.
10. Karpinski, J.; Jun, J.; Porowski, S. *J. Cryst. Growth* **1984**, *66*, 1.
11. Akasaki, I.; Amano, H.; Murakami, H.; Sassa, M.; Kato, H.; Manabe, K. *J. Cryst. Growth* **1993**, *128*, 379.
12. Lei, T.; Moustakas, T. D.; Graham, R. J.; He, Y.; Berkowitz, S. J. *J. Appl. Phys.* **1992**, *71*, 4933.
13. Kobayashi, A.; Asai, T.; Kawai, S.; Chong, P. J. *MRS Symp. Proc.*; Boston, Symp. Proc.: **1990**, 158, 91; CHEMICA '90, Auckland, Conf. Proc.: **1990**, 462.
14. Kim, S. H.; Hwang, J. S.; Chong, P. J.; Choi, J. G. *71st Annual Meeting Kor. Chem. Soc.* **1993**, 47.
15. Suto, M.; Lee, L. C. *J. Chem. Phys.* **1983**, *78*, 4515.
16. Vere, A. W.; Rodway, D. C.; Mackey, K. J.; Smith, P. C.; Moores, P. K. *J. Cryst. Growth* **1992**, *121*, 62.
17. Lee, S. S.; Park, S. M.; Chong, P. J. *J. Mater. Chem.* **1993**, *3*, 347.
18. Kawabata, T.; Matsuda, T.; Koike, S. *J. Appl. Phys.* **1984**, *15*, 2367.

Nonstoichiometry of the Terbium Oxide

Chul Hyun Yo, Kwang Sun Ryu, Eun Seok Lee*, and Keu Hong Kim

Department of Chemistry, Yonsei University, Seoul 120-749
**Department of Chemistry, ChungJu University, ChungJu 360-764*
Received July 29, 1993

The x values of nonstoichiometric chemical formula, $Tb_4O_{7-\delta}$ or $TbO_{1.5+x}$, have been determined in temperature range from 600℃ to 1000℃ under oxygen partial pressure of 2×10^{-1} to 1×10^{-5} atm by using quartz microbalance. The x values varied from 0.0478 to 0.1964 in the above conditions. The enthalpy of formation for x' in $TbO_{1.5+(0.25-x_0-x')}$, ΔH_f, was 4.93-3.40 kcal mol^{-1} and the oxygen partial pressure dependence was $-1/8.80\sim-1/11.8$ under these conditions. The electrical conductivity of the $TbO_{1.5+x}$ was measured under the same conditions and the values varied from about 10^{-3} to 10^{-6} $\Omega^{-1}cm^{-1}$ within semiconductor range. The activation energies for the conduction increase with oxygen partial pressure from 0.83 to 0.89 eV under the above conditions. The $1/n$ values obtained from the oxygen pressure dependence of the conductivity are 1/4.4-1/5.2. The conduction mechanism, defect structure, and other physical properties of the oxides are dicussed with the x values, the electrical conductivity values, and the thermodynamic data.

Introduction

The terbium-oxygen and the praseodymium-oxygen systems have many similarities for physical properties[1]. Tb_4O_7 is dark brown or black solid and contains the equal amounts of Tb^{3+} and Tb^{+4}. It dissolves in hot concentrated acids with formation of salts and loses oxygen on heating.

In the terbium-oxygen system, there are many phases with compositions $TbO_{1.500}$, $TbO_{1.714}$, $TbO_{1.816}$, $TbO_{1.830}$ and TbO_2. Hyde and Eyring[2] have suggested that these phases belong to a homologous series of Tb_nO_{2n-2}. Tb_2O_3 possesses the C-type structure up to about 1500℃ while TbO_2 crystalized with the fluorite structure. The $TbO_{1.5+x}$ may contain excess oxygen where x may have a value up to 0.1 at temperatures of 950-1000℃ at 500-600 torr O_2.

Vasil'eva *et al*[3]. showed the plot of -RT ln P_{O_2} *vs* composition with isotherms and phase regions indicated. Kordis and Eyring[4] reported a partial phase diagram which was derived from an isobaric study using high-temperature X-ray diffraction. They have also confirmed some of the isobaric and isothermal tensiometric studies[5] with a sample (TbO_x) of greater purity.

The electrical conductivity for rare earth oxides has been studied[6,7,8]. Subba Rao *et al*[8]. suggested that an electrical conductivity maximum occurs at $TbO_{1.75}$, and the result is interpreted in terms of the hopping model and the small polaron theory. The oxide is a p-type semiconductor in the $TbO_{1.5}$-$TbO_{1.75}$ range and an n-type semiconductor in the $TbO_{1.75}$-TbO_2.

These earlier studies did not include a quantitative evaluation of the relationship between the nonstoichiometric composition and the electrical conductivity. The objective of the present study is to determine the high temperature defect structure of the pure Tb_4O_7 by means of the weight change and electrical conductivity measurements. The electrical conductivity is closely related to the nonstoichiometric compositions of the oxides, and a combination of these measurements gives informations on the defect structure and conduction mechanism. The thermodynamic properties and conduction mechanism of terbium oxide shall be discussed with the nonstoichiometry, the enthalpy of formation of x', the oxygen partial pressure dependence of x', the activation energy of the electrical conductivity, and the oxygen partial pressure dependence of the electrical conductivity.